



# Synthesis, properties and uses of ZnO nanorods: a mini review

Peyman K. Aspoukeh<sup>1</sup> · Azeez A. Barzinjy<sup>2,3</sup> · Samir M. Hamad<sup>1</sup>

Received: 26 March 2021 / Accepted: 25 July 2021  
© Islamic Azad University 2021

## Abstract

Zinc oxide (ZnO) nanorods have been extensively investigated, owing to their extraordinary applications in numerous fields, spatially microchip technology, solar cells, sensors, photodetectors, photocatalysts and many others. Recently, using ZnO nanorods, as photocatalysts, are receiving increasing attention in environmental defense applications. This mini review summarizes some remarkable applications for ZnO nanorods. First, the various chemical and physical procedures that were used to produce ZnO nanorods are identified through symmetric matrices and heterogeneous structures, then the authors explain how to use these methods to produce ZnO nanorods. This mini review, also, discusses the applications of ZnO nanorods in many fields, especially in field release, emission properties, and electron transference. Last but not least, the appropriate conclusions for future research using ZnO nanorods have been successfully explained.

**Keywords** ZnO nanorods · Vapor phase process · MOCVD process · Luminescence · Field emission · Gas sensor · Field effect transistors

## Introduction

Nanomaterials are bases of nanoscience and nanotechnology. Based on the number of dimensions nanomaterials can be classified into zero, one, two and three dimensions (Fig. 1). One dimensional (1D) nanomaterials in this sequences are the most significant materials due to their attractive physical characteristics. One dimensional nanomaterials, essentially, possess three different structures, namely nanorods, nanowires and nanotube. In 1D, one dimension is exterior from the nanoscale. While, in two dimensional nanomaterials (2D), two dimensions are exterior from the nanoscale. This type displays plate like profiles and comprises graphene, nanofilms, nano-layers, and nano-coatings. Lastly, three dimensional nanomaterials (3D) are materials that are not limited to the nanoscale in any lengths. This type can comprise bulk

powders, dispersals of nanoparticles, packages of nanowires, and nanotubes as well as multi nano-layers [1].

1D nanomaterials are lengthened in one precise direction [2]. These type of nanomaterials are leading the analogs 2D and 3D due to their exclusive optical and electronic properties. Semiconducting ZnO nanorods are of vital attention for the growth of devices in Nano-electronics, chemical and biological sensing, energy conversion and storage, photovoltaic cells, batteries, capacitors, hydrogen-storage devices, light-emitting diodes, catalysis, drug delivery, and piezoelectric energy nano-generation [3].

Nanorods exceed the other structures since it can be made from most elements, i.e. metals/nonmetals and compounds, and the artificial requests for their fabrication are much easier than the other structures [4]. A great number of researchers are interested in nanorods owing to their exceptional chemical and physical characterization as well as wide application in electronic devices [5–7]. Essential researches, on what happens when the size of materials approaches to the nanoscale, i.e. 1–100 nm, indicating that they possess, considerably, dissimilar characteristics than the equivalent materials at bulk scale. Moreover, fabricating electronic nanodevices is not an easy process [8, 9]. Nowadays, there are numerous electronic devices that have been thought to be out of reach for the last decades [10, 11]. Among the dissimilar methods that have been utilized for synthesizing whiskers or

✉ Azeez A. Barzinjy  
azeez.azeez@su.edu.krd

<sup>1</sup> Scientific Research Centre, Soran University, 44008 Soran, Iraq

<sup>2</sup> Department of Physics, College of Education, Salahaddin University-Erbil, Erbil, Iraq

<sup>3</sup> Physics Education Department, Faculty of Education, Tishk International University, Erbil, Iraq



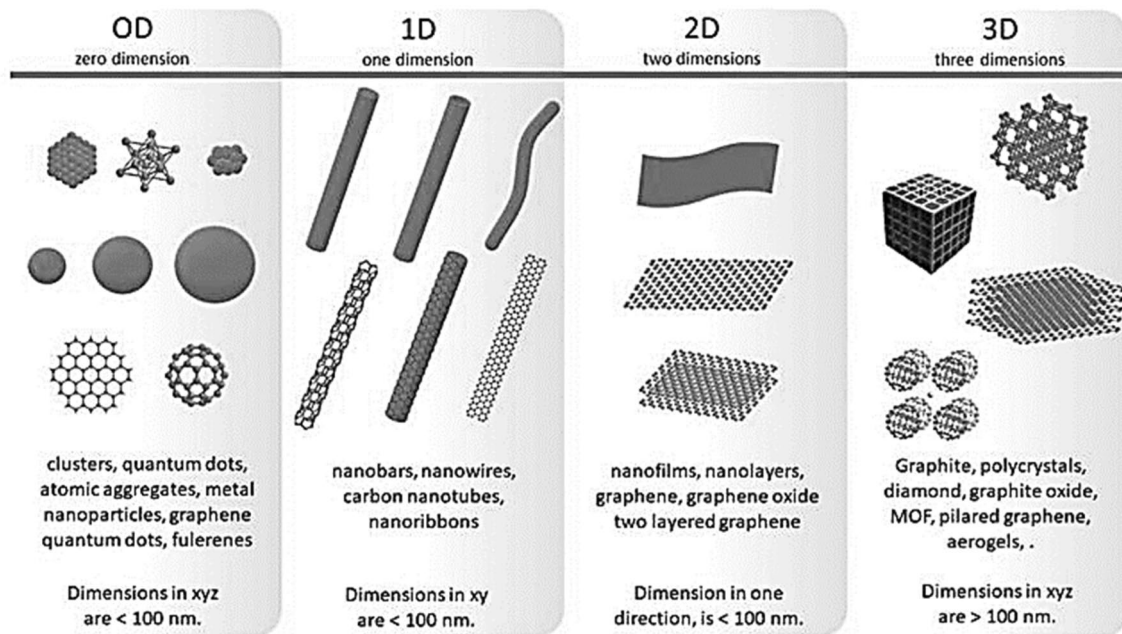


**Fig. 1** Classification of nanostructures materials: zero dimension (0D), one dimension (1D), two dimension (2D), and three dimension (3D)

fibers, the vapor–solid [12] and Vapor–liquid–solid [13–15] techniques have been used more than the other forms. These methods are useful in synthesizing semiconducting materials like doped heterojunctions and molecular crystals of group II–VI and III–V [16, 17]. In addition to the available methods for producing one-dimensional nanostructured materials, such as template-induced growth [18–20], laser ablation-catalytic growth [21, 22], solution–liquid–solid growing in carbon-based diluters [20, 23, 24], metal carbon-based chemical-vapor-deposition [25], and oxide based growth [26, 27], other approaches to produce one-dimensional nanostructures are also available.

The exciton binding energy for ZnO is 60 MeV, and it has a bandgap energy of 3.5 eV. The ZnO film is transparent to light, absorbs UV rays, and produces a piezoelectric response. Additionally, ZnO is compatible with other atoms and it has potential uses in medicine. Investigation has established that the morphology of one-dimensional ZnO nanostructured materials affects their optical and electrical properties [28, 29]. It can be stated that, 1D nanostructured ZnO is the most productive among other dimensions, due to its simplicity of fabrication and use in electronics applications. As shown in Fig. 2, one-dimensional ZnO possesses several structures, such as nanobelts, nanonails, nanodots, nanotubes, nanorods, and nanowires [30–32].

Nowadays, carbon nanotubes (CNT) have been one of the greatest progressive useful supplies owing to their higher electronic characterization, noble thermal and chemical steadiness, extraordinary mechanical power, and outsized surface area [34]. In recent times, the ZnO-CNT amalgams

and mixture nanostructures have been deliberated as a capable nominee for refining the device competence in the electronic and optoelectronic procedures since these constructions can offer the improved electrical and optical characterization through the supportive physical interface among ZnO nanostructures and CNT [35].

On the other hand, with the speedy growing of electronics and telecommunication activities, electromagnetic contamination is a dangerous issue to be studied since it not only touches the sympathy and performance of the devices but also disturbs human's healthiness. At this point, lightweight cross composite mats has been reported this possess high porosity and it composed from zinc oxide nanorods, amorphous carbon, and nickel zinc ferrite for outstanding electromagnetic interference (EMI) shielding in the X-band. This combination leads to better magnetic loss of the electromagnetic waves [36].

This mini review article provides an overview of recent developments of ZnO nanorods. The presentation was arranged to discuss the existing methods for producing ZnO nanorods. The novelty of this mini review can be highlighted here, since this review provides a brief description of the most important uses of ZnO nanorods and highlights their use in many fields. Also, this review describes the most important proposals, future and scientific trends in this field to illuminate the path of researchers. ZnO nanorods synthesis and applications is a quite broad area of research, therefore the limitations of this study is the authors cannot cover all of the details spatially within this mini review. Owing to the exceptional properties of ZnO nanorods it has



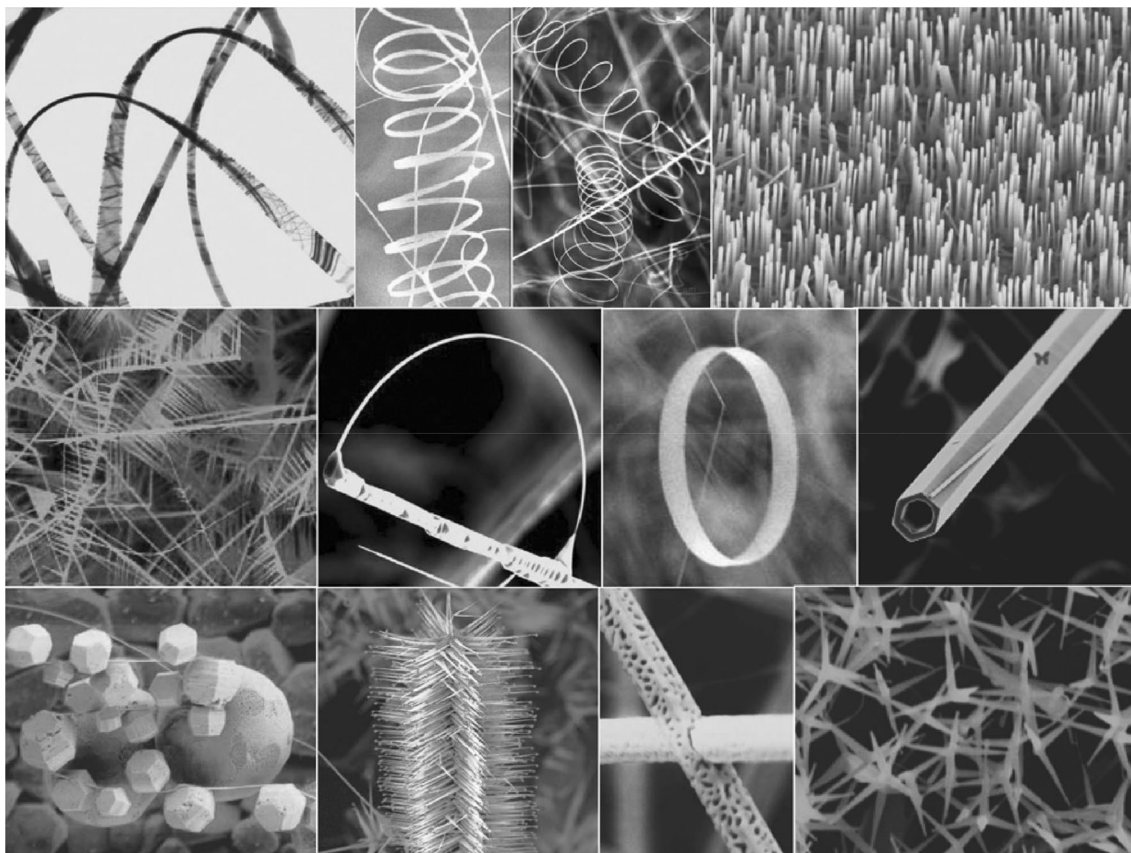


**Fig. 2** Different forms of ZnO powders using thermal evaporation [33]

numerous potential applications for instance photo-catalysis, solar cells, sensors, and generators. Amongst the requests of ZnO nanorods, photo-catalysis is progressively used for ecological protection. Additional investigation is desired to increase the feature of ZnO nanorods and large scale yield ZnO nanorods for applied manufacturing requests. Based on this mini review, ZnO nanorods is likely to be one of the most significant supplies in photo-catalytic along with others applications.

## Growth of ZnO nanorods

### The vapor-phase process

One of the crucial procedures for creating 1D nanorod structure is the thermal evaporation (vapor phase) method [37]. It is still uncertain for researchers what method is best for fabricating ZnO nanorods. Initially, the vapor is generated by evaporation, chemical reaction, and gas reaction. The specific vapor gets rapidly heated up and then gradually cooled on the substrate [38] to provide piles of nanomaterial. Some researchers manufactured nanorods

with the evaporation of ZnO commercial powder [39, 40]; others synthesized ZnO nanowire-nanoribbon junction crossover arrays [41, 42]. Although the vapor-phase procedure is easy and straight, heating the commercial mixture powder  $\text{SnO}_2$  and ZnO, but it has to be done on extremely high temperature. It is essential to analyses the additional reactions and breakdown to this process. ZnO nanorods vapor-phase synthesis reported by Gundiah et al. utilizing a carbothermic process [43]. They stated that, as soon as ZnO is reduced by carbon in a flowing reactor, Zn vapor will form and it can be conveyed to the growing region, then will be reduced to Zn once again [43]. Other authors stated that ZnO nanorods and nanowires can be prepared by oxidizing Zn at high temperatures i.e. between 500 and 550 °C [44, 45]. Wagner and Ellis, for the first time, demonstrated how a catalytic process could be used to produce micrometer-scale whiskers by means of gold as a catalytic-agent [46]. Also, in a typical gas-liquid-solid reaction system, first the reactants can be dissolved in to nano size dewdrops of a metallic catalytic-agent then the distinct crystalline-rods are grown. This technique has been utilized, enormously, to produce ZnO nanorods [16, 47].



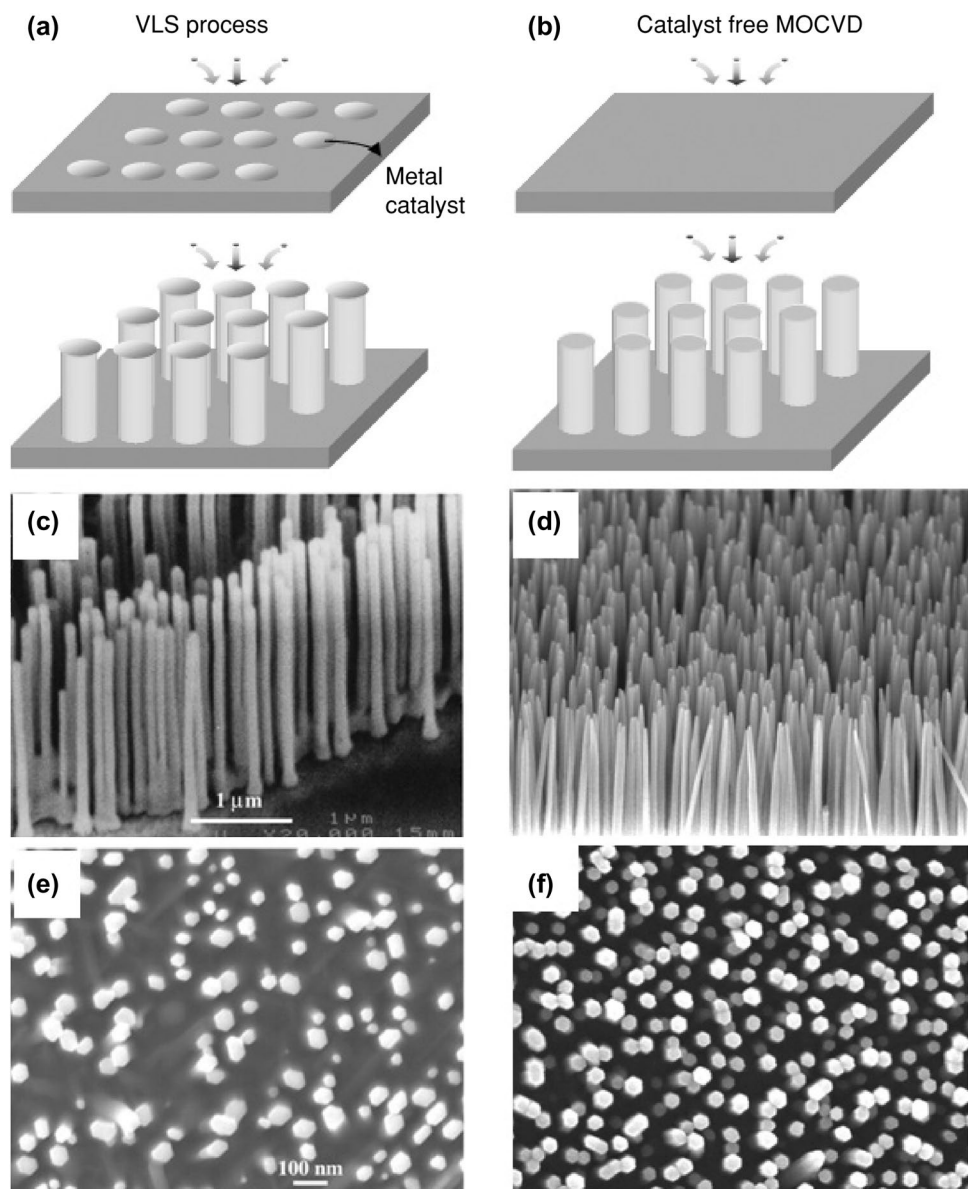
## The MOCVD process

ZnO nanorods are typically, in many cases, grown up by metal organic chemical-vapor-deposition (MOCVD). Originally, MOCVD has been utilized to produce ZnO quantum dots and thin films [48–50]. Nevertheless, MOCVD progress has been recently investigated to grow zinc oxide nanorods using the free catalytic-agent MOCVD process as demonstrated in Fig. 3 [51, 52]. ZnO nanorods created in this process were pure and contained no impurities or external catalysts. In addition, the formation of ZnO nanorods and other related topics have been reported in other studies intensely [53–56]. Similarly, the catalyst-free process has been studied, and the main reason for this type of growth is said to be due to a lack of anisotropic

surface energy in wurtzite structures. Moreover, for the turbulent flow of high-speed laminar gas flow arrays, the reactant gases are adsorbed onto the needle tip. Since the nanorods tips have a larger surface area, the growth rate will be relatively faster [57].

This catalyst-free method is not only applicable for the fabrication of anisotropic crystals, it can be utilized also for the fabrication of nanostructures [58–60]. The catalyst-free MOCVD is also a promising method for cultivation of ZnO nanorods with a temperature between 400 and 500 °C which is basically far away from that expected in growing catalytic based nanowire, i.e. 900 °C [61]. Fabrication of ZnO nanorods at a low temperature, will offer greater power and versatility making them a candidate for usage in photonic nanoscale and microelectronic procedures [62].

**Fig. 3** The growth of ZnO nanorod is indicated by schematic diagrams **a** VLS and **b** MOCVD free of catalysts. **c**, **e** Are the SEM graph of VLS grown up ZnO nanorods and **d**, **f** are the SEM graph of MOCVD grown up ZnO nanorods [63]



## The chemical method

Hydrothermal synthesis method is another common technique to produce ZnO nanorods [64–67]. Other chemical methods have been utilized for ZnO nanorods fabrication, such as aqueous-solution [68], bio mineralization [69], along with sol–gel method [70]. O’Brien et al. have described a new synthesis technique for ZnO nanorods production [71]. They utilized zinc acetate in the thermal decomposition of an organic oleic acid solvent to produce ZnO nanorods with a monodisperse in normal length of 40–50 nm with a diameter of 2 nm.

## Production of ZnO nanorods collections

Perpendicularly high-oriented arrangements of nanorods through a constant distribution of dimension and thickness can be defined as nanorods arrays. Nanorods are among the important topics in nanotechnology due to their high potential applications and they account as a building blocks in nanodevices [72]. As illustrated in Fig. 3, ZnO nanorods arrays were synthesized with a solid substratum by applying the vapor–liquid–solid (VLS) method and using a metal like gold [73, 74]. Another method of manufacturing catalyst-free was used to grow ZnO nanorods aligned to them [59, 75]. Recently, a new low temperature method for cultivating ZnO nanorods (Fig. 3) with catalyst-free MOCVD is reported by Yi et al. [63, 76].

## ZnO heterostructures nanorods growing

One dimensional heterostructures nanorods is one of the most useful techniques in the production of many new electronic devices, spatially in a micrometer scale [77–79]. The structures of nano superlattice have recently grown by multiple vapor-phase semiconductor reactants [80–86]. The core of this model was displayed by the growth of a structure of a silicone nanowire or carbon nanotube [87]. This method can be successfully applied for a metal catalyst with two different material. Superlattices up to 20 sheets of GaAs in addition to GaP have been compositionally modeled [88]. Also, p–n modulated junction nanometrics made by chemical vapor or laser-assisted catalytic growth have been prepared. Wu et al. reported that Si/SiGe superlattices are being produced utilizing an amalgam pulsed laser removal/chemical-vapor-deposition (PLA-CVD) method [82]. Bjork et al. also manufactured a time period of 100 to only several nanometers of InAs/InP nano-superlattices. The use of a high-vacuum chamber for chemical beam epitaxy techniques was similar to metal-catalyzed nanowire growth technologies [83–85]. Moreover, Bjork et al. also investigated single-electron tunneling behaviors and electrical transport properties. They analyzed resonant tunneling between InAs

and InP nanowire structures which can be produced when InAs being sandwiched between InP barriers.

In place of the traditional method described by Yi et al., Zhang et al. proposed the mixed interfacial layer [89, 90]. Metallic and semiconducting Nanostructured materials play essential roles in the electronic contacts in many nanosize devices [91]. Yi et al. described how decreasing the thickness of the Ni layer in a nanorod heterostructure leads to the decreasing of the boundary between ferromagnetism and superparamagnetism [90]. In a recent study, scientists discovered that amorphous of  $\text{Al}_2\text{O}_3$  layers have been formed on ZnO nanorods through atomic-layer deposition (ALD) [92–94]. In an epitaxial-molding attitude [95] and metallic-organic vapor epitaxy (MOVPE) [96], Goldberger et al. and Ann et al. have validated the preparation of GaN/coaxial ZnO nanorod heterostructure. The heterostructures bring inconceivable tools, containing field-effect transistors along with HEMTs, that are made of coaxial nano-nanorods [97]. These hollow nanotubes can be utilized for electrophoresis of nanocapillaries and biochemical sensor nanosubstances [98].

## Nanorods quantum structures

In addition to possessing multiple novel physical properties, nanorods structure have some quantum mechanical properties. To study these novel properties, a number of techniques, such as MBE and MOVPE, have been developed [4, 99, 100]. The catalytic-assisted vapor–liquid–solid assisted technique for manufacturing the compositionally modulated nanowires. However, a relatively broad hetero-interface leads to the production of a quantum structure with an ultra-thin quantum-well layer, then the structure becomes extremely hard to synthesize [101]. Yi et al. have produced quantum structures, without using catalytic ZnO/ $\text{Zn}_{0.8}\text{Mg}_{0.2}\text{O}$ , through utilizing MOVPE [102]. Nanorods manifold quantum-well (MQW) illustrations with 1.1 nm and 2.5 nm wells using TEM and also photoluminescence spectra (PL) spectra, respectively, are shown on Fig. 4.

Figure 4 shows spectra layers in multiple quantum wells of ZnO/ $\text{Zn}_{0.8}\text{Mg}_{0.2}\text{O}$  layers. Since lighter elements are less dispersed in a z-contrast image (Fig. 4), the ZnO layers are lighter than the  $\text{ZnO}/\text{Zn}_{0.8}\text{Mg}_{0.2}\text{O}$ . These heterostructures display the perfect inscription of the quantum-confinement and an increased black column change with a diminishing coating width. Similarly, as illustrated in Fig. 4, the PL bands of sequence of ZnO/ $\text{Zn}_{0.8}\text{Mg}_{0.2}\text{O}$  MQW nanorods arrangements display radiation energies reliant upon the potential well thicknesses. Other research concludes that widening well widths leads to a drop in the blue-shifting value [103]. This change can be ignored at a weighted threshold of 110 Å. The theoretical calculation in ten periods shows that random decreasing width of the potential



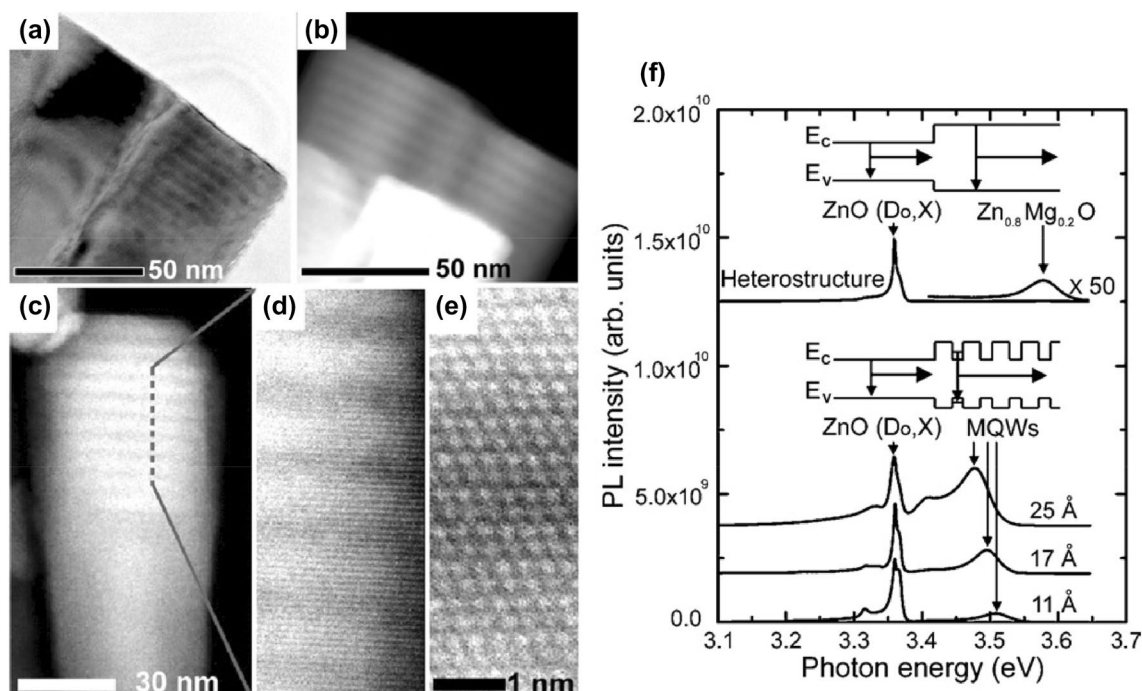


**Fig. 4** ZnO/Zn<sub>0.8</sub>Mg<sub>0.2</sub>O MQW nanorods TEM pictures and PL spectrums. **a** Low size TEM graph of the 2.5 nm wells example. **b**, **e** Z-distinction descriptions with an increasing magnification of the

2.5 nm fine width example. **f** The ZnO/Zn<sub>0.8</sub>Mg<sub>0.2</sub>O and ZnO/Zn<sub>0.8</sub>Mg<sub>0.2</sub>O nanorods band arrays were presented in 10 K PL spectra (ZnO/Zn<sub>0.8</sub>Mg<sub>0.2</sub>O) [102]

well produces an increase in the amount of PL emission. In addition, the optical features of individual quantum-well structures (SQWs) would give insight into the ZnO/ZnMgO nanorods structures (SNOM) [104]. The exchanging procedures is desirable for the nanophotonic tools [105]. Yatsui et al. calculated space and spectrally resulted photoluminescence graphing of separate nanorods SQWs [106]. In the case of ZnO/ZnMgO nanorods SQW, the spectrum SNOM PL shows the band substantial in the ground-state and the resulting excited primary-holes (Fig. 5).

These studies approves the remark of the quantum-confinement consequence in nanorods quantum wells. A blue shift takes place, in the nanorods structures within the band-edge PL, as a result of a quantum-confinement effect. However, no quantum-confinement consequence was observed in the radiating path for widths of nanorods larger than 20 nm. This is more likely due to the large concentration of electrons and holes in zinc oxide, and the smaller Bohr exciton (1.25 nm) [107]. To observe the quantum-confinement behavior in ZnO nanorods, their nanorods should be less than 10 nm in diameter. Recently, Wang et al. [108] investigated the quantum-confinement effects in ultra-thin ZnO nanostructures and Park et al. [109] investigated and grew ultrafine ZnO nanostructures. Wang et al. used a tinny Sn film in place of a reagent and manufactured the ultra-thin ZnO nanobelts with typical and a standard deviation of  $6 \pm 1.5$  nm [108]. The emission peak of nanobelts experience

a blue shift when the width of nanobelt has been reduced. This shift most probably results from the quantum-confinement. Park et al. through using catalyst-free MOCVD method synthesized ZnO nanorods with a widths fewer than 10 nm [109]. The high resolution transmission electron microscope image shows that the ZnO nanorods through widths near to 8 nm, possess a blue shift in the PL peak owing to the quantum-confinement consequence (Fig. 6). Decreasing the diameter in the nanorods causes a blue shift in the PL peak position.

Moreover, Yi et al. have synthesized the Zn<sub>1-x</sub>Mg<sub>x</sub>O coaxial-nanorods quantum assemblies, through multiple coatings Zn<sub>1-x</sub>Mg<sub>x</sub>O sheets. ZnO/Zn<sub>0.8</sub>Mg<sub>0.2</sub>O coaxial-nanorods quantum assemblies showed a reduction in thermal quenching and growth in PL intensity. The quantum structures permit the formation of specific potential profiles in the heterostructures. This construction has a valuable advantages in the atomic-scale electronic devices such as field-effect transistors as well as organic LEDs [110].

### ZnO nanorods alloys and doping

It can be comprehend that, adding divalent elements to the cation site will modify the ZnO bandgap. Doping with magnesium (Mg) can increase the bandgap energy of ZnO-based compounds between 3.4 to about 4.0 eV, besides doping with cadmium (Cd) can decrease the bandgap to  $\sim 3.0$  eV



**Fig. 5** **a** ZnO/ZnMgO nanorod SQW Monochromatic PL picture achieved with 3.483 eV photon energy. **b** Spot X cross-sectional PL profile. **c** Solid-curves show ZnO/ZnMgO nanorod SQWs close-field PL spectrum at different excitation thicknesses oscillating between 1 and 12 W cm<sup>-2</sup>. The far-field PL spectrum is shown by the dashed-curves (F1 and F2). Every spectrum was achieved at 15 K. **d** API of 3.48 eV (open-circles) and 3.508 eV (open-circles) (closed-circles) [105]

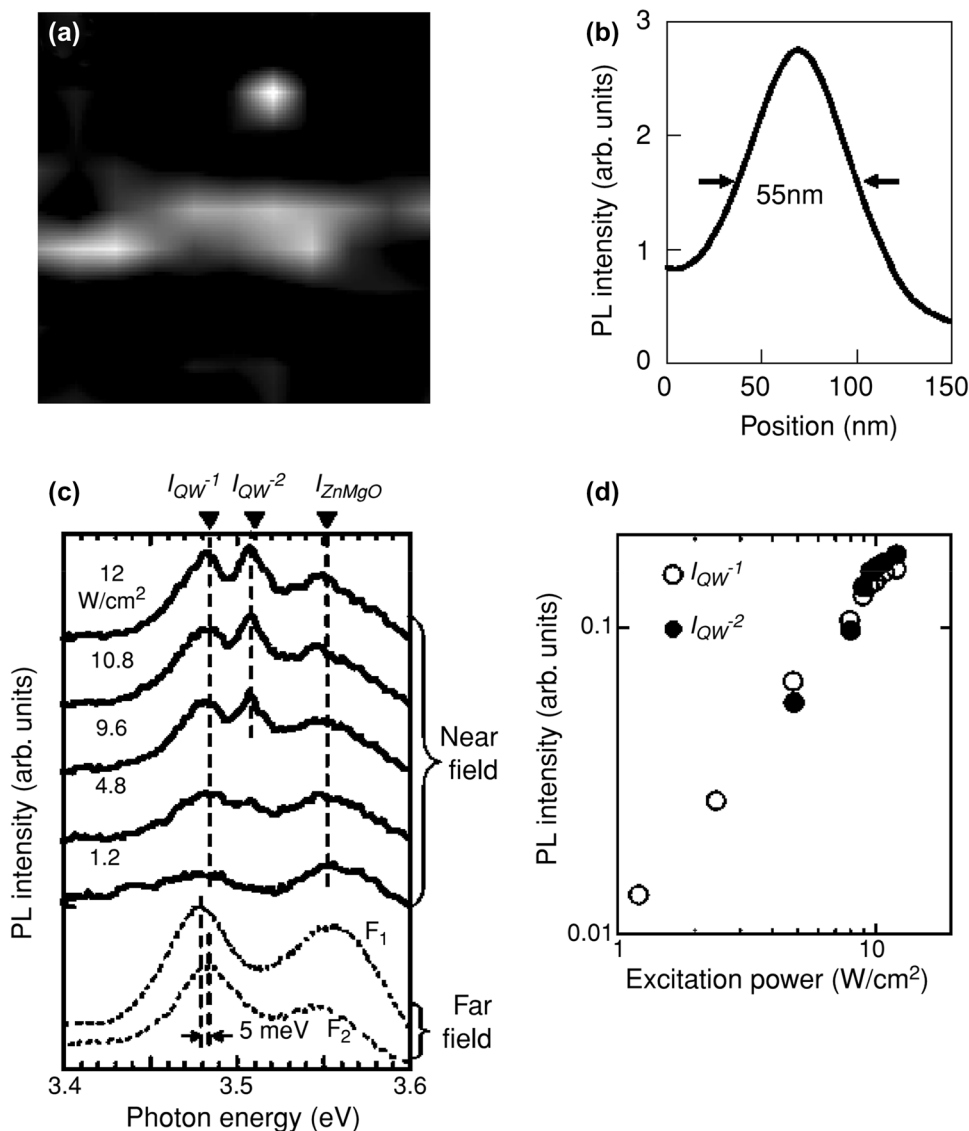
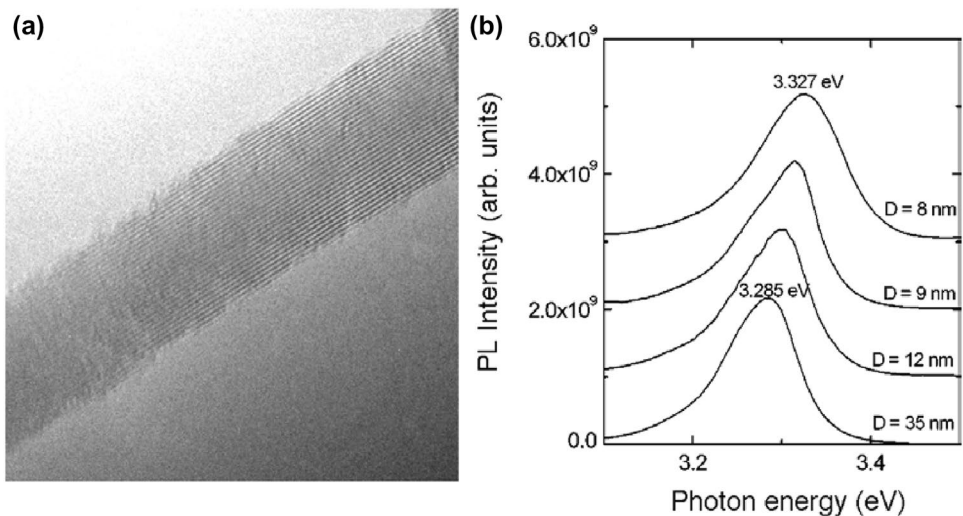


**Fig. 6** **a** Extraordinary resolution ZnO TEM graphs through a regular width of 8 nm. **b** and ZnO spectra with different regular width (*D*) of 8, 9, 12 and 4 nm. PL spectra with different average diameter. Reproduces from [109]



[111, 112]. Geng et al. [113], through a modest physical vaporization method, and Bae et al. [114], through applying chemical-vapor-deposition, synthesized the S-doped ZnO nanowires. Wan et al. [115] described Cd-doped growth at 900 °C through vaporizing metallic Zn and Cd. Chang et al. manufactured  $Zn_{1-x}Mn_xO$  magnetic diluted semiconductor nanorods via vapor-phase growth [116]. On the other hand, Mn, Co-doped ZnO nanorods by means of molecular-beam-epitaxy was synthesized by Ip et al. [117]. Indeed, ZnO is naturally an n-type semiconductor, so the conductivity of ZnO is controllable by doping. To prepare Ga-doped ZnO nanorods, a pulse laser can be utilized [118]. The synthesizing of p-type ZnO is a challenge owing to high n-type carrier concentration [119–121]. Nevertheless, There are several efforts regarding the preparation of p-type ZnO epitaxial thin films, but there is a lack of information about the synthesizing of p-type ZnO nanorods and wires [122].

## Properties and applications of ZnO nanorods

Due to their distinctive characteristics, ZnO semiconductor nanorods are desirable apparatuses for nanoscale applications, spatially in electronic and photonic devices. For instance a number of ZnO nanorods devices such as ultraviolet photodetectors [123–126], sensors [127–129], light-emitting device arrays [130–132] field consequence transistors [133–135], intra-molecular p–n junction diode [136, 137] and Schottky diode [138–140] have been manufactured recently.

## Luminescence

Currently, progress has been done in accommodating the bulk ZnO single crystal photoluminescence spectrum. Several groups of researchers described how different luminescence peaks were produced at a given location [141–145].

Concerning the analysis of single nanowires, the PL's primary laser beam's lateral resolution is limited to approximately one micrometer as a result of visual restrictions. Consequently, greatest number of ZnO nanoparticle PL ranges remained acquired on numerous arbitrarily rotated or allied nanoparticles [147–151].

The room temperature luminescence of ZnO nanorods exhibits a single wide-ranging peak. Currently, this peak is too short to provide enough information about the reactive recombination process associated with the low temperature photoluminescence of ZnO bulk single-crystals [152–154]. Until now, there have been few experiments on ZnO nanowires at low temperature of photoluminescence [145, 155, 156]. Yi et al. [146] studied the permitted exciton and three donor bound excitation ranges of extraordinary

pure ZnO nanorods arrangements at 10 K as shown in Fig. 7. On the other hand, as displayed in Fig. 8, room temperature UV radiation was produced with a threshold power density below on hundred  $\text{kW cm}^2$  [157, 158]. Choy et al. [159] found that ZnO nanorods arrays' possess high UV radiation efficiency on silicon wafers and also on an aluminum oxide substrate [157].

Yu et al. [160] intensively discussed the arbitrary laser stroke with intelligible response in ZnO nanorods arrays placed on ZnO layers. Compared to phosphorescence, cathodic-luminescence is a much more valuable method, especially in the mapping of nanoscale sized constructions. Lorenz et al. found that the CL spectrum depended only slightly on the PL spectrum of ZnO nanowires [161]. ZnO is a good material for narrow wavelength photonic requests, but p–n dopants in the ZnO make construction of ZnO p–n homojunction procedures difficult [162].

## Field radiation

Field radiation cathodes is another attracted components owing to their possible requests in power devices and flat sheet spectacles. Considerably, much research has been done recently to fabricate nanorods arrangements of field emitters. In this review, spinet type metal pine cone development beforehand the discovery of the carbon nanotubes (CNTs) will be discussed [163]. Nano-sized carbon fibers have a

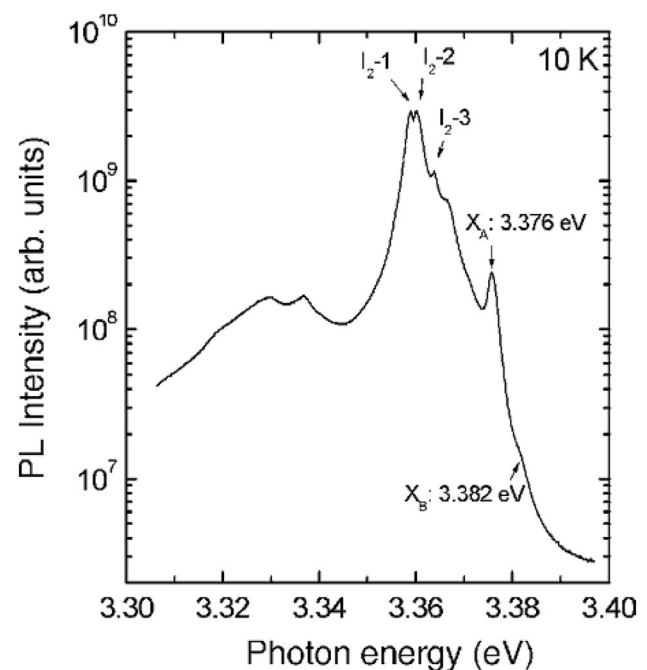
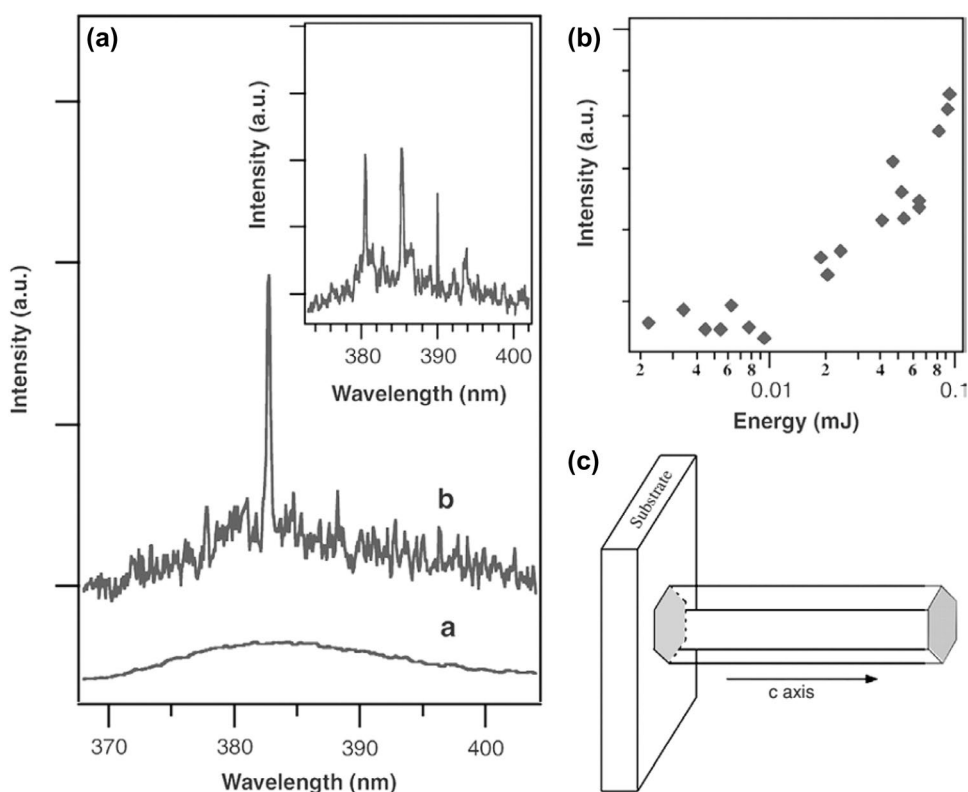


**Fig. 7** ZnO nanorods measured at 10 K PL spectrum of high quality. The dominant near-band emission is four different peaks with a maximum width of 3.359, 3.360, 3.364, and 3.376 eV with full width of 1–3 meV (FWHM) [146]



**Fig. 8** **a** Radiation spectra from the lasing inception from the nanowire array underneath (line a) and overhead (line b and inclusion). These spectra have a pump capacity of 20, 100 and 150  $\text{kW cm}^{-2}$ . **b** Integrated nanowire emitting intensity in function of the energy intensity of the visual pushing. **c** Representation diagram of the resonance cavity of a nanowire through two certainly facing hexagonal end faces that act as mirrors



diameter of several hundred nanometers and a few micrometers. The ratio between the length of the nanowire and its width makes it an excellent candidate for synthesizing an extraordinary electric field at the landfills of carbon nanotubes for electron emission at reasonable smeared energies. Numerous reports have demonstrated that the CNTs emit easily detectable radiation. The manufacture of vertically aligned CNT collections for field-emission procedures is however not simple. One of the challenges to be addressed is the degradation, in addition to oxygen, of residual gases from CNT field emitters to prepare high achievements field-emission displays (FEDs) [164].

Once 1D ZnO nanostructure is synthesized a large number of investigators suggested that such nanostructures could be utilized in producing bases as they possess big aspect-ratios like CNT, which could decrease the squalor of field-emission appearances caused by remaining gas [165]. As shown in Fig. 9, Lee et al. demonstrated the first field-emission experiments from ZnO nanowires [166]. The experiments employed a range of ZnO nanowires. Although there was little vertical alignment of ZnO nanowires, the turning and threshold fields is about  $6.0 \text{ V } \mu\text{m}^{-1}$  at a current density of  $0.1 \mu\text{A cm}^{-2}$  and  $11.0 \text{ V } \mu\text{m}^{-1}$  at current density  $0.1 \text{ mA cm}^{-2}$  respectively [166].

Even though these field emissions properties are lesser than CNTs, they are sufficiently acceptable to be used for the usage of electron emitters, i.e. turn-on field of  $1 \text{ V } \mu\text{m}^{-1}$

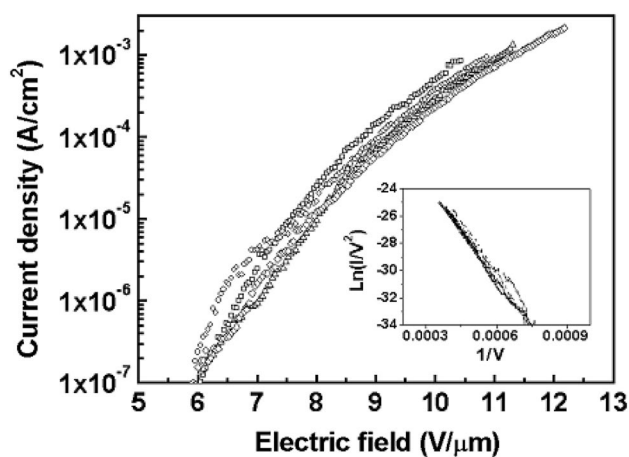


**Fig. 9** Current ZnO emission density nanoparticles developed on the substrate of silicone at 550. Inset reports the Fowler–Nordheim behavior in the field emission [166]. Instead of a p-ZnO system, p-GaN used for homojunction, Yi et al. [167] due to a comparable basic energy bandgap and the crystal structure of the n-ZnO/pGaN electroluminescent (EL) tools

and field-emission current of  $1.5 \text{ mA}$  at  $3 \text{ V } \mu\text{m}^{-1}$ ; current density,  $J = 90 \mu\text{A cm}^{-2}$  [168]. Shortly after that, several scientists reported that a range of ZnO nanowires and nanorods were being issued on electron emission [169, 170]. The results have shown that the features of 1D ZnO nanostructures field emission are comparable to CNTs.



The ZnO nanoneedle arrays' vertical alignment examined by investigators to the analysis of the electron emission foundation with 1D ZnO nanostructures. ZnO aligned nanoneedle arrays affect field emissions since electrostatic models have been checked in metallic seed case by a hypothetical control [171]. Various approaches have been settled for the production of perpendicularly aligned nanowires and field-emission testing. In addition, Li et al. described the vertical alignment effect on field-emission features [172].

The morphological effect of the nanorods tip on the electric fields is crucial to consider, since high-pitched tips growth the efficient electric field at the tips [173]. In general, for the needlelike structures the field-emission features of 1D ZnO nanostructures are better. Li et al. have stated that ZnO nanoneedles' tip surface disturbances play a vital role in improving field-emission features [174]. Xu et al. also described the good field emitting characterization of ZnO nanopins with a  $1.9 \text{ V } \mu\text{m}^{-1}$  turn-on field at the current density of  $0.1 \text{ } \mu\text{A cm}^{-2}$  [175]. Specifically, owing to the very high-pitched tips, ZnO nanoneedle arrangements could be used for electron emitters [176, 177]. There has been substantial attention in field experiments on 1D ZnO nanostructures emissions.

Other groups conducted several tests on doping 1D ZnO nanostructures and they proposed that raises in electrical conductivity with incapitating would improve ZnO 1D nanostructures' field-emission features [178]. Xu et al. showed that Gallium doping enhances ZnO nanofibre arrays' field-emission characteristics and Jo et al. also reported that ZnO nanofibre field-emission characteristics could also be improved with hydrogen annealing [179–181]. 1D nanostructures ZnO are viewed by many researchers as good field emitters. The modern researches on 1D ZnO nanostructures conducted as field emitters, so that their field-emission features were not sufficiently adjusted [169]. Future testing on numerous characteristics, such as electrical conduct, density regulator, and instrument constructions can, however, produce outstanding field emitters built upon 1D ZnO nanostructures [182, 183].

## Gas detecting

Nanostructured ZnO have been very attractive for stationary gas sensors, whose ultra-high surface-to-volume ratio gives them great potential to overcome fundamental limitations [149, 184–186]. Some research groups have recently examined the gas identifying features of ZnO nanowires [187, 188]. Wang et al. observed that the current of Cd-doped ZnO nanowire increases when irradiated in humid air to 95% this can be used for detecting moisture. Zinc oxide based microelectromechanical systems demonstrated an extraordinary compassion to ethanol gas, with a surprisingly quick reply time of 10 s.

Yi et al. demonstrated that ZnO nanowires can be used as humidity sensors at high temperatures, they also showed that ZnO nanorods displayed promising applications as biological sensors at low temperatures [189]. Nanosensors and single crystalline ZnO nanorods can be used in bimolecular preparation, catalyst-free metal organic vapor-phase epitaxy method [190, 191]. Other methods such as lithography for e-beams are useful for manufacturing metal micro patterns on one ZnO nanorods. Once the ZnO electronic biosensors with biotin modification were introduced to streptavidin, their conductance will significantly increase. It specifies that ZnO nanosensors have a high electrical sensitivity to biological species detection [192].

## Electron transport properties

For the new research, the electron transport properties of microscale devices are vital. Harnock et al. have confirmed that ZnO nanorods are non-linear and asymmetric in current–voltage ( $I$ - $V$ ) with asymmetry factor of more than 25 at a 3 V bias voltage [193]. Lee et al. examined a medial resistivity of ZnO nanowire and showed that the regular resistivity was around one order of extent above uncovered single ZnO nanowires in anodic aluminum oxide (AAO) templates [194]. In recent years, ZnO-based nanodevice such as diodes, p-n junctions, field-effect transistors (FETs), ZnO nanostructure-based electroluminescent and Schottky have been investigated by many researchers [138–140, 195].

The ZnO nanobelts were deposited in a 120 nm thick- $\text{SiO}_2$  gate dielectric/Si substrate on predetermined gold electrode arrays for the production of field-effect transistors [196]. As inception of the ZnO nanobelt field-effect transistor presented an onset voltage of 15V, a swapping relation of approximately 100, and a peak conductivity of  $1.25 \times 10^3 \text{ cm}$  was shown in Fig. 10. The performance characteristics of ZnO nanobelt transistor is identical to that of carbon nanotubes on Au electrodes or Ti electrodes [197]. Park et al. have recently developed high enactment ZnO nanorods FETs which have suggestively developed FET features with 105 high current on-/off ratios and  $1.8 \text{ } \mu\text{S}$  [198]. In addition, a maximum of  $1000\text{--}1200 \text{ cm}^2\text{V}^{-1} \text{ s}^{-1}$  was observed in the electron mobility calculated from trans conductance. The high enactment nanoscale FETs acquired demonstrate ZnO Nanorods' feasibility for electronic nanodevices [199].

Yi et al. have also used another method for manufacturing the ZnO-based device. They produced nanorods heterostructures vertically aligned metal/semiconductor (M/SC) only through vaporizing metal onto ZnO nanorods tips [84]. As indicated in Fig. 11, Au/ZnO nanorods showed corrective  $I$ - $V$  representative curves deprived of substantial opposite biases up to  $-8 \text{ V}$ . Additionally, Au/Ti/ZnO nanorods showed rectilinear  $I$ - $V$  characteristics, representing ohms in the form of ZnO nanorods. The rise of the carriers at the

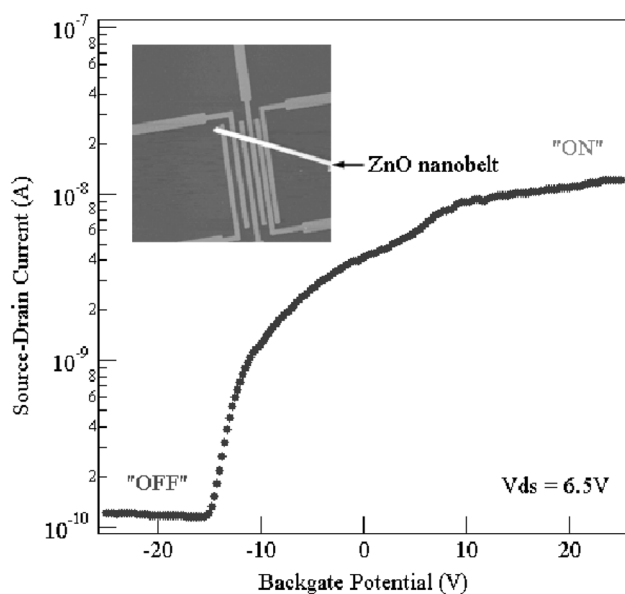


**Fig. 10** Current source-drain versus ZNO nanobelt FET gate bias in the environment. AFM ZnO FET image on golden electrodes (inset) [200]

interface resulted in the ohmic behavior of nanorods heterostructures in Au/Ti/ZnO. This result demonstrates that ultra-high-density nanorods and Schottky nanodevice arrays can be applied to ZnO nanorods [201].

## Conclusion

This study is a mini review on the recent researches on ZnO nanorods with distinct concentration on its potential applications. The authors reviewed the semiconducting photocatalysts and deliberated a selection of production approaches of ZnO nanorods and their resultant value in photocatalysis. The mechanism of synthesizing ZnO nanorods with their advantages and disadvantages has been investigated intensively. Although, a lot of progress in this field has been made recently, but still some challenges have remained. In fact, the first challenge was in all applied methods, the ZnO nanorods are assembled randomly together to produce complex structures or devices. The second challenge was the problematical issues in the growing p-type ZnO nanorods. As a result of the exclusive material characterization, ZnO nanorods are important for several possible applications for instance photocatalysis, solar cells, sensors, and many other devices. Amongst the uses of ZnO nanorods, photocatalysis is being progressively utilized for ecological safety. Additional investigation is desirable to expand the superiority of ZnO nanorods and across-the-board yield ZnO nanorods for applied

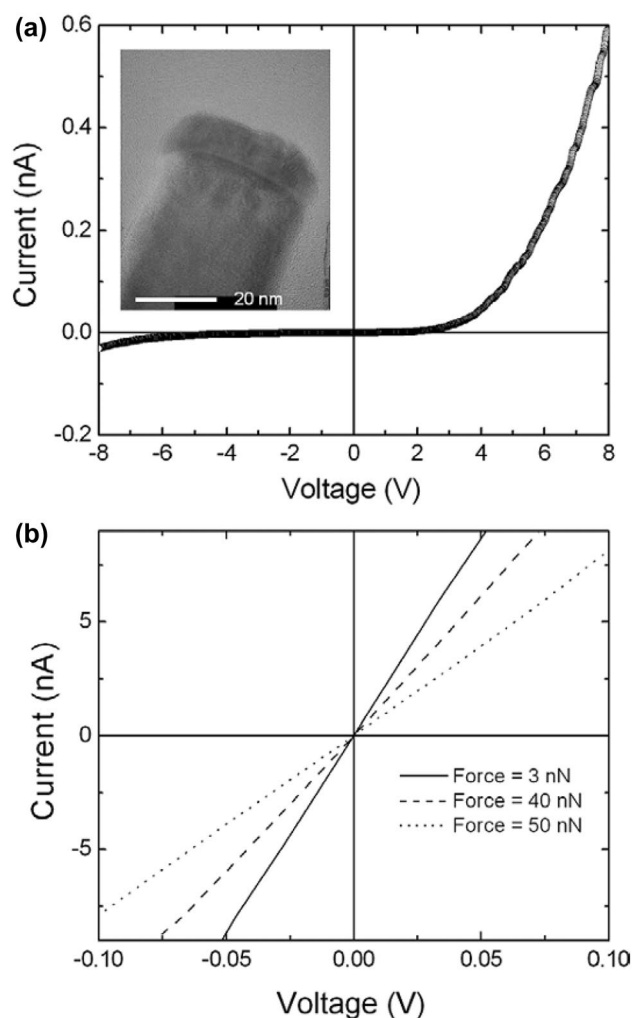


**Fig. 11** Typical  $I$ - $V$  curves of the characteristic heterostructures **a** Au/ZnO, and **b** Au/Ti/ZnO, indicating Schottky and ohmic conduct. Inset displays a TEM of the Au/ZnO [202]

manufacturing requests. According to this mini review, it is more likely that ZnO nanorods could be a good candidate for the most necessary materials in photocatalysis as well as other applications. Thus, extra investigation is anticipated to rise the feature of ZnO nanorods and large scale yield ZnO nanorods for applied manufacturing needs.

**Acknowledgements** The authors thank Salahaddin University-Erbil, Tishk International University and Soran University for their unconditional supports. A sincere thank goes to Dr David M.W. Waswa at Tishk International University for his diligent proofreading of this manuscript.

**Funding** This research received no external funding.

## Declarations

**Conflicts of interest** The authors declare no conflict of interest.

## References

- Pokropivny, V., Skorokhod, V.: Classification of nanostructures by dimensionality and concept of surface forms engineering in nanomaterial science. *Mater. Sci. Eng., C* **27**(5–8), 990–993 (2007)
- Su, B., Wu, Y., Jiang, L.: The art of aligning one-dimensional (1D) nanostructures. *Chem. Soc. Rev.* **41**(23), 7832–7856 (2012)
- Li, B.L., et al.: Low-dimensional transition metal dichalcogenide nanostructures based sensors. *Adv. Func. Mater.* **26**(39), 7034–7056 (2016)
- Ghassan, A.A., Mijan, N.-A., Taufiq-Yap, Y.H.: Nanomaterials: an overview of nanorods synthesis and optimization. In: *Nanorods and Nanocomposites*, Chapter 2, vol. 11, no. 11, pp. 8–33. IntechOpen (2020)
- Abdulrahman, A.F., et al.: Fabrication and Characterization of High-Quality UV Photodetectors Based ZnO Nanorods Using Traditional and Modified Chemical Bath Deposition Methods. *Nanomaterials* **11**(3), 677 (2021)
- Lebepe, T.C., Parani, S., Oluwafemi, O.S.: Graphene oxide-coated gold nanorods: synthesis and applications. *Nanomaterials* **10**(11), 2149 (2020)
- Pellas, V., et al.: Gold Nanorods for LSPR biosensing: synthesis, coating by silica, and bioanalytical applications. *Biosensors* **10**(10), 146 (2020)
- Frascaroli, J., et al.: Resistive switching in high-density nanodevices fabricated by block copolymer self-assembly. *ACS Nano* **9**(3), 2518–2529 (2015)
- Fried, J.P., et al.: Challenges in fabricating graphene nanodevices for electronic DNA sequencing. *MRS Communications* **8**(3), 703–711 (2018)
- Euler, H.-C.R., et al.: A deep-learning approach to realizing functionality in nanoelectronic devices. *Nat. Nanotechnol.* **15**(12), 992–998 (2020)
- Rajendran, J., et al.: Nano meets security: Exploring nanoelectronic devices for security applications. *Proc. IEEE* **103**(5), 829–849 (2015)
- Yamai, I., Saito, H.: Vapor phase growth of alumina whiskers by hydrolysis of aluminum fluoride. *J. Cryst. Growth* **45**, 511–516 (1978)
- Wagner, R.: Vapor-liquid-solid mechanism of Single crystal growth. *Appl. Phys. Lett.* **4**, 89–90 (1964)
- Klimovskaya, A., Ostrovskii, I., Ostrovskaya, A.: Influence of growth conditions on morphology, composition, and electrical properties of n-Si wires. *Phys. Status Solidi (a)* **153**(2), 465–472 (1996)
- Okabe, T., Nakagawa, M.: Growth of  $\alpha$ -Ag<sub>2</sub>S whiskers in a VLS system. *J. Cryst. Growth* **46**(4), 504–510 (1979)
- Zhang, X., Wu, D., Geng, H.: Heterojunctions based on II-VI compound semiconductor one-dimensional nanostructures and their optoelectronic applications. *Curr. Comput.-Aided Drug Des.* **7**(10), 307 (2017)
- Liu, M., et al.: Twin-induced one-dimensional homojunctions yield high quantum efficiency for solar hydrogen generation. *Nat. Commun.* **4**(1), 1–8 (2013)
- Han, W., et al.: Synthesis of gallium nitride nanorods through a carbon nanotube-confined reaction. *Science* **277**(5330), 1287–1289 (1997)
- Wang, C., et al.: Synthesis of novel SbSI nanorods by a hydrothermal method. *Inorg. Chem. Commun.* **4**(7), 339–341 (2001)
- Ma, D., et al.: Cu-In<sub>2</sub>S<sub>3</sub> nanorod induced the growth of Cu&In co-doped multi-arm CdS hetero-phase junction to promote photocatalytic H<sub>2</sub> evolution. *Chem. Eng. J.* **399**, 125785 (2020)
- Labis, J.P., et al.: Designing zinc oxide nanostructures (nanoworms, nanoflowers, nanowalls, and nanorods) by pulsed laser ablation technique for gas-sensing application. *J. Am. Ceram. Soc.* **102**(7), 4367–4375 (2019)
- Park, H., et al.: Synthesis of ultra-small palladium nanoparticles deposited on CdS nanorods by pulsed laser ablation in liquid: role of metal nanocrystal size in the photocatalytic hydrogen production. *Chem. A Eur. J.* **23**(53), 13112–13119 (2017)
- Jiang, Y., et al.: Elemental solvothermal reaction to produce ternary semiconductor CuInE<sub>2</sub> (E= S, Se) nanorods. *Inorg. Chem.* **39**(14), 2964–2965 (2000)
- Wang, C., et al.: Preparation and Photoluminescence of CaS: Bi, CaS: Ag, CaS: Pb, and Sr<sub>1-x</sub>Ca<sub>x</sub>S Nanocrystallites. *J. Electrochem. Soc.* **150**(3), G163 (2003)
- Ameen, S., et al.: Vertically aligned ZnO nanorods on hot filament chemical vapor deposition grown graphene oxide thin film substrate: solar energy conversion. *ACS Appl. Mater. Interfaces.* **4**(8), 4405–4412 (2012)
- Murkute, P., et al.: Emerging material zinc magnesium oxide based nanorods: Growth process optimization and sensor application towards humidity detection. *Sens. Actuators B Chem.* **256**, 204–216 (2018)
- Willander, M., et al.: Zinc oxide nanorod based photonic devices: recent progress in growth, light emitting diodes and lasers. *Nanotechnology.* **20**(33), 332001 (2009)
- Mydeen, S.S., et al.: Biosynthesis of ZnO nanoparticles through extract from *Prosopis juliflora* plant leaf: Antibacterial activities and a new approach by rust-induced photocatalysis. *J. Saudi Chem. Soc.* **24**(5), 393–406 (2020)
- Li, X., et al.: Effects of free electrons and quantum confinement in ultrathin ZnO films: a comparison between undoped and Al-doped ZnO. *Opt. Express* **21**(12), 14131–14138 (2013)
- Ding, M., et al.: One-dimensional zinc oxide nanomaterials for application in high-performance advanced optoelectronic devices. *Curr. Comput.-Aided Drug Des.* **8**(5), 223 (2018)
- Yildirim, O.A., Liu, Y., Petford-Long, A.K.: Synthesis of uniformly distributed single- and double-sided zinc oxide (ZnO) nanocombs. *J. Cryst. Growth* **430**, 34–40 (2015)
- Senthilkumar, N., et al.: Synthesis of ZnO nanorods by one step microwave-assisted hydrothermal route for electronic device applications. *J. Mater. Sci. Mater. Electron.* **29**(4), 2927–2938 (2018)
- Wang, Z.L.: Nanostructures of zinc oxide. *Mater. Today* **7**(6), 26–33 (2004)
- Ghalandari, M., et al.: Applications of nanofluids containing carbon nanotubes in solar energy systems: a review. *J. Mol. Liq.* **313**, 113476 (2020)
- Khairy, M., Naguib, E.M., Mohamed, M.M.: Enhancement of photocatalytic and sonophotocatalytic degradation of 4-nitrophenol by ZnO/graphene oxide and ZnO/carbon nanotube nanocomposites. *J. Photochem. Photobiol. A Chem.* **396**, 112507 (2020)
- Gupta, S., et al.: Hybrid composite mats composed of amorphous carbon, zinc oxide nanorods and nickel zinc ferrite for tunable electromagnetic interference shielding. *Compos. B Eng.* **164**, 447–457 (2019)
- Srivatsa, K., Chhikara, D., Kumar, M.S.: Synthesis of aligned ZnO nanorod array on silicon and sapphire substrates by thermal evaporation technique. *J. Mater. Sci. Technol.* **27**(8), 701–706 (2011)
- Navale, Y., et al.: NO<sub>2</sub> Gas Sensor Based on ZnO Nanorods Synthesised by Thermal Evaporation Method, in *Techno-Societal 2018*, pp. 315–321. Springer (2020)
- Chrissanthopoulos, A., et al.: Synthesis and characterization of ZnO/NiO p-n heterojunctions: ZnO nanorods grown on NiO thin film by thermal evaporation. *Photon. Nanostruct.-Fundam. Appl.* **9**(2), 132–139 (2011)
- Li, Y., et al.: ZnO microcolumns originated from self-assembled nanorods. *J. Mater. Sci.* **43**(5), 1711–1715 (2008)

41. Quan, L.N., et al.: Nanowires for photonics. *Chem. Rev.* **119**(15), 9153–9169 (2019)
42. Baratto, C., et al.: On the alignment of ZnO nanowires by Langmuir-Blodgett technique for sensing application. *Appl. Surf. Sci.* **528**, 146959 (2020)
43. Gundiah, G., et al.: Carbothermal synthesis of the nanostructures of Al<sub>2</sub>O<sub>3</sub> and ZnO. *Top. Catal.* **24**(1–4), 137–146 (2003)
44. Kurbanov, S., et al.: Photoluminescence properties of ZnO nanorods synthesized by different methods. *Semiconductors* **52**(7), 897–901 (2018)
45. Khanlary, M.R., Vahedi, V., Reyhani, A.: Synthesis and characterization of ZnO nanowires by thermal oxidation of Zn thin films at various temperatures. *Molecules* **17**(5), 5021–5029 (2012)
46. Peng, X., Wickham, J., Alivisatos, A.: Kinetics of II–VI and III–V colloidal semiconductor nanocrystal growth: “focusing” of size distributions. *J. Am. Chem. Soc.* **120**(21), 5343–5344 (1998)
47. Wang, X., Peng, Q., Li, Y.: Interface-mediated growth of monodispersed nanostructures. *Acc. Chem. Res.* **40**(8), 635–643 (2007)
48. Mei, T., Hu, Y.: Synthesis, self-assembly and optoelectronic properties of monodisperse ZnO quantum dots. In: *Optoelectronic Devices and Properties*, Chapter 11, pp. 215–240 (2011)
49. Wang, D., et al.: Interfacial emission adjustment in ZnO quantum dots/p-GaN heterojunction light-emitting diodes. *J. Phys. Chem. C* **119**(5), 2798–2803 (2015)
50. Hao, Q.: Improved manufacturing processes for better materials properties—from quantum dots to bulk materials. *ES Mater Manuf* **8**, 1–2 (2020)
51. Lan, S., et al.: Morphology and optical properties of zinc oxide thin films grown on Si (100) by metal-organic chemical vapor deposition. *J. Mater. Sci.: Mater. Electron.* **20**(1), 441–445 (2009)
52. Jung, I.O., Park, J.Y., Kim, S.S.: Substrate dependent growth modes of ZnO nanorods grown by metalorganic chemical vapor deposition. *J. Cryst. Growth* **355**(1), 78–83 (2012)
53. Kim, D.C., et al.: ZnO nanorod arrays grown on glass substrates below glass transition temperature by metalorganic chemical vapor deposition. *J. Mater. Sci.: Mater. Electron.* **20**(1), 245–248 (2009)
54. Kim, A.-Y., et al.: Effects of temperature on ZnO hybrids grown by metal-organic chemical vapor deposition. *Mater. Res. Bull.* **47**(10), 2888–2890 (2012)
55. Lei, P.-H., Cheng, C.-H.: Fabrication of Ag nanoparticle/ZnO thin films using dual-plasma-enhanced metal-organic chemical vapor deposition (DPEMOCVD) system incorporated with photoreduction method and its application. *Mater. Sci. Semicond. Process.* **57**, 220–226 (2017)
56. Swathi, S., et al.: Branched and unbranched ZnO nanorods grown via chemical vapor deposition for photoelectrochemical water-splitting applications. *Ceram. Int.* **47**(7), 9785–9790 (2021)
57. Kim, J.Y., et al.: Tailoring the surface area of ZnO nanorods for improved performance in glucose sensors. *Sens. Actuators B Chem.* **192**, 216–220 (2014)
58. Montenegro, D., et al.: Non-radiative recombination centres in catalyst-free ZnO nanorods grown by atmospheric-metal organic chemical vapour deposition. *J. Phys. D Appl. Phys.* **46**(23), 235302 (2013)
59. Ray, P.G., et al.: Surfactant and catalyst free facile synthesis of Al-doped ZnO nanorods—An approach towards fabrication of single nanorod electrical devices. *Appl. Surf. Sci.* **512**, 145732 (2020)
60. Mani, G.K., Rayappan, J.B.B.: Selective recognition of hydrogen sulfide using template and catalyst free grown ZnO nanorods. *RSC Adv.* **5**(68), 54952–54962 (2015)
61. Rusli, N.I., et al.: Growth of high-density zinc oxide nanorods on porous silicon by thermal evaporation. *Materials* **5**(12), 2817–2832 (2012)
62. Khan, W., et al.: Induced photonic response of ZnO nanorods grown on oxygen plasma-treated seed crystallites. *Nanomaterials* **8**(6), 371 (2018)
63. Park, W.I., et al.: Metalorganic vapor-phase epitaxial growth of vertically well-aligned ZnO nanorods. *Appl. Phys. Lett.* **80**(22), 4232–4234 (2002)
64. Ocakoglu, K., et al.: Microwave-assisted hydrothermal synthesis and characterization of ZnO nanorods. *Spectrochim. Acta Part A Mol. Biomol. Spectrosc.* **148**, 362–368 (2015)
65. Motevalizadeh, L., Heidary, Z., Abrishami, M.E.: Facile template-free hydrothermal synthesis and microstrain measurement of ZnO nanorods. *Bull. Mater. Sci.* **37**(3), 397–405 (2014)
66. Sutradhar, S., et al.: Effect of hydrothermal synthesis on physical property modulation and biological activity of ZnO nanorods. *Mater. Res. Express* **6**(12), 125077 (2020)
67. Gan, Y.X., et al.: Hydrothermal synthesis of nanomaterials Hindawi. Springer (2020)
68. Ungula, J., Swart, H.: Study on the role of growth time on structural, morphological and optical properties of un-capped and L-cyst.-capped ZnO nanorods grown on a GZO seeded thin film layer from an aqueous solution. *J. Alloys Compd.* **821**(459p), 153459 (2020)
69. Vidya, C., et al.: Photo-assisted mineralisation of titan yellow dye using ZnO nanorods synthesised via environmental benign route. *SN Appl. Sci.* **2**(4), 1–15 (2020)
70. Farha, A.H., Al Naim, A.F., Mansour, S.A.: Thermal Degradation of Polystyrene (PS) Nanocomposites Loaded with Sol Gel-Synthesized ZnO Nanorods. *Polymers* **12**(9), 1935 (2020)
71. Yin, M., et al.: Zinc oxide quantum rods. *J. Am. Chem. Soc.* **126**(20), 6206–6207 (2004)
72. Stagon, S.P., Huang, H.: Syntheses and applications of small metallic nanorods from solution and physical vapor deposition. *Nanotechnol. Rev.* **2**(3), 259–267 (2013)
73. Moumen, A., et al.: One dimensional ZnO nanostructures: Growth and chemical sensing performances. *Nanomaterials* **10**(10), 1940 (2020)
74. Alvi, N., et al.: Influence of different growth environments on the luminescence properties of ZnO nanorods grown by the vapor–liquid–solid (VLS) method. *Mater. Lett.* **106**, 158–163 (2013)
75. Kim, D., Leem, J.-Y.: Catalyst-free synthesis of ZnO nanorods by thermal oxidation of Zn films at various temperatures and their characterization. *J. Nanosci. Nanotechnol.* **17**(8), 5826–5829 (2017)
76. Park, W.I., et al.: ZnO nanoneedles grown vertically on Si substrates by non-catalytic vapor-phase epitaxy. *Adv. Mater.* **14**(24), 1841–1843 (2002)
77. Goswami, L., et al.: Graphene quantum dot-sensitized ZnO-nanorod/GaN-nanotower heterostructure-based high-performance UV photodetectors. *ACS Appl. Mater. Interfaces.* **12**(41), 47038–47047 (2020)
78. Chang, J.S., et al.: Exploration of a novel Type II 1D-ZnO nanorods/BiVO<sub>4</sub> heterojunction photocatalyst for water depollution. *J. Ind. Eng. Chem.* **83**, 303–314 (2020)
79. Bai, L., Mei, J.: Low amount of Au nanoparticles deposited ZnO nanorods heterojunction photocatalysts for efficient degradation of p-nitrophenol. *J. Sol-Gel Sci. Technol.* **94**, 468–476 (2020)
80. Lauhon, L.J., et al.: Epitaxial core–shell and core–multishell nanowire heterostructures. *Nature* **420**(6911), 57–61 (2002)
81. Gudiksen, M.S., et al.: Growth of nanowire superlattice structures for nanoscale photonics and electronics. *Nature* **415**(6872), 617–620 (2002)



82. Wu, Y., Fan, R., Yang, P.: Block-by-block growth of single-crystalline Si/SiGe superlattice nanowires. *Nano Lett.* **2**(2), 83–86 (2002)
83. Björk, M., et al.: One-dimensional heterostructures in semiconductor nanowhiskers. *Appl. Phys. Lett.* **80**(6), 1058–1060 (2002)
84. Björk, M., et al.: Nanowire resonant tunneling diodes. *Appl. Phys. Lett.* **81**(23), 4458–4460 (2002)
85. Thelander, C., et al.: Single-electron transistors in heterostructure nanowires. *Appl. Phys. Lett.* **83**(10), 2052–2054 (2003)
86. Macaluso, R., et al.: Progress in violet light-emitting diodes based on ZnO/GaN heterojunction. *Electronics* **9**(6), 991 (2020)
87. Yusof, J.M., et al.: Effect of zinc oxide nucleation on flexible bio based carbon nanotube cotton via chemical bath deposition method. *Microelectron. Eng.* **234**, 111439 (2020)
88. Kovalenko, M.V., et al.: Prospects of nanoscience with nanocrystals. *ACS Nano* **9**(2), 1012–1057 (2015)
89. Park, W.I., et al.: Metal-ZnO heterostructure nanorods with an abrupt interface. *Jpn. J. Appl. Phys.* **41**(11A), L1206 (2002)
90. Jung, S.W., et al.: Fabrication and controlled magnetic properties of Ni/ZnO nanorod heterostructures. *Adv. Mater.* **15**(16), 1358–1361 (2003)
91. Theerthagiri, J., et al.: A review on ZnO nanostructured materials: energy, environmental and biological applications. *Nanotechnology* **30**(39), 392001 (2019)
92. Chaaya, A.A., et al.: Tuning optical properties of Al<sub>2</sub>O<sub>3</sub>/ZnO nanolaminates synthesized by atomic layer deposition. *J. Phys. Chem. C* **118**(7), 3811–3819 (2014)
93. Li, S., et al.: Interface engineering of high efficiency perovskite solar cells based on ZnO nanorods using atomic layer deposition. *Nano Res.* **10**(3), 1092–1103 (2017)
94. Romo-Garcia, F., et al.: Optoelectronic attenuation behavior of Al<sub>2</sub>O<sub>3</sub>/ZnO nanolaminates grown by Atomic Layer Deposition. *Thin Solid Films* **669**, 419–424 (2019)
95. Goldberger, J., et al.: Single-crystal gallium nitride nanotubes. *Nature* **422**(6932), 599–602 (2003)
96. An, S.J., et al.: Heteroepitaxial fabrication and structural characterizations of ultrafine GaN/ZnO coaxial nanorod heterostructures. *Appl. Phys. Lett.* **84**(18), 3612–3614 (2004)
97. Yoon, I.T., Cho, H.D.: Two-step preparation and characterization of ZnO Core–Si shell coaxial nanorods. *Journal of Theoretical and Applied Physics* **14**(1), 9–16 (2020)
98. Adam, V., Vaculovicova, M.: Nanomaterials for sample pretreatment prior to capillary electrophoretic analysis. *Analyst* **142**(6), 849–857 (2017)
99. Shen, J., et al.: Insight into the Ga/In flux ratio and crystallographic plane dependence of MBE self-assembled growth of InGaN nanorods on patterned sapphire substrates. *Nanoscale* **12**(6), 4018–4029 (2020)
100. Chu, Y.-L., et al.: Characteristics of gas sensors based on co-doped ZnO nanorod arrays. *J. Electrochem. Soc.* **167**(11), 117503 (2020)
101. Jen, Y.-J., et al.: Deposited ultra-thin titanium nitride nanorod array as a plasmonic near-perfect light absorber. *Sci. Rep.* **10**(1), 1–12 (2020)
102. Park, W.I., et al.: Quantum confinement observed in ZnO/ZnMgO nanorod heterostructures. *Adv. Mater.* **15**(6), 526–529 (2003)
103. Parra, M.R., Haque, F.Z.: Structural and optical properties of poly-vinylpyrrolidone modified ZnO nanorods synthesized through simple hydrothermal process. *Optik* **125**(17), 4629–4632 (2014)
104. Kuang, D., et al.: Dual-ultraviolet wavelength photodetector based on facile method fabrication of ZnO/ZnMgO core/shell nanorod arrays. *J. Alloys Compd.* **860**, 157917 (2021)
105. Yatsui, T., et al.: Evaluation of the discrete energy levels of individual ZnO nanorod single-quantum-well structures using near-field ultraviolet photoluminescence spectroscopy. *Appl. Phys. Lett.* **85**(5), 727–729 (2004)
106. Ohtsu, M., et al.: Nanophotonics: design, fabrication, and operation of nanometric devices using optical near fields. *IEEE J. Sel. Top. Quantum Electron.* **8**(4), 839–862 (2002)
107. Kumar, S.G., Rao, K.K.: Zinc oxide based photocatalysis: tailoring surface-bulk structure and related interfacial charge carrier dynamics for better environmental applications. *RSC Adv.* **5**(5), 3306–3351 (2015)
108. Wang, X., et al.: Large-scale synthesis of six-nanometer-wide ZnO nanobelts. *J. Phys. Chem. B* **108**(26), 8773–8777 (2004)
109. Park, W.I., et al.: Quantum confinement observed in ultrafine ZnO and ZnO/Zn/sub 0.8/Mg/sub 0.2/O coaxial nanorod heterostructures. In: 4th IEEE Conference on Nanotechnology, vol. 11, pp. 83–85 (2004)
110. Li, T., Goldberger, J.E.: Atomic-Scale Derivatives of Solid-State Materials. *Chem. Mater.* **27**(10), 3549–3559 (2015)
111. Sirkeli, V., Hartnagel, H.L.: ZnO-based terahertz quantum cascade lasers. *Opto-Electron. Rev.* **27**(2), 119–122 (2019)
112. Mondal, S., Mitra, P.: Preparation of cadmium-doped ZnO thin films by SILAR and their characterization. *Bull. Mater. Sci.* **35**(5), 751–757 (2012)
113. Geng, B., et al.: Synthesis and optical properties of S-doped ZnO nanowires. *Appl. Phys. Lett.* **82**(26), 4791–4793 (2003)
114. Bae, S.Y., Seo, H.W., Park, J.: Vertically aligned sulfur-doped ZnO nanowires synthesized via chemical vapor deposition. *J. Phys. Chem. B* **108**(17), 5206–5210 (2004)
115. Wan, Q., et al.: Positive temperature coefficient resistance and humidity sensing properties of Cd-doped ZnO nanowires. *Appl. Phys. Lett.* **84**(16), 3085–3087 (2004)
116. Chang, Y., et al.: Synthesis, optical, and magnetic properties of diluted magnetic semiconductor Zn 1-x Mn x O nanowires via vapor phase growth. *Appl. Phys. Lett.* **83**(19), 4020–4022 (2003)
117. Ip, K., et al.: Ferromagnetism in Mn- and Co-implanted ZnO nanorods. *J. Vac. Sci. Technol. B Microelectron. Nanometer Struct. Process. Meas. Phenom.* **21**(4), 1476–1481 (2003)
118. Yan, M., et al.: Self-assembly of well-aligned gallium-doped zinc oxide nanorods. *J. Appl. Phys.* **94**(8), 5240–5246 (2003)
119. Gautam, S.K., et al.: Giant enhancement of the n-type conductivity in single phase p-type ZnO: N thin films by intentionally created defect clusters and pairs. *Solid State Commun.* **218**, 20–24 (2015)
120. Thakur, I., et al.: Facile synthesis of single crystalline n-/p-type ZnO nanorods by lithium substitution and their photoluminescence, electrochemical and photocatalytic properties. *New J. Chem.* **39**(4), 2612–2619 (2015)
121. Singh, B.K., Tripathi, S.: pn homojunction based on Bi doped p-type ZnO and undoped n-type ZnO for optoelectronic application in yellow-red region of visible spectrum. *J. Lumin.* **198**, 427–432 (2018)
122. Kwon, D.-K., Porte, Y., Myoung, J.-M.: Fabrication of ZnO nanorods p–n homojunction light-emitting diodes using Ag film as self-doping source for p-type ZnO nanorods. *J. Phys. Chem. C* **122**(22), 11993–12001 (2018)
123. Gu, P., Zhu, X., Yang, D.: Vertically aligned ZnO nanorods arrays grown by chemical bath deposition for ultraviolet photodetectors with high response performance. *J. Alloys Compd.* **815**, 152346 (2020)
124. Yatskiv, R., Grym, J., Verde, M.: Graphite/ZnO nanorods junction for ultraviolet photodetectors. *Solid-State Electron.* **105**, 70–73 (2015)
125. Zhou, H., et al.: Ultraviolet photodetectors based on ZnO nanorods-seed layer effect and metal oxide modifying layer effect. *Nanoscale Res. Lett.* **6**(1), 1–6 (2011)



126. Ji, Y., et al.: Ultraviolet photodetectors using hollow p-CuO nanospheres/n-ZnO nanorods with a pn junction structure. *Sens. Actuators A Phys.* **304**, 111876 (2020)
127. Huang, J., et al.: Visible light-activated room temperature NH<sub>3</sub> sensor base on CuPc-loaded ZnO nanorods. *Sens. Actuators B Chem.* **327**, 128911 (2021)
128. Wang, H., et al.: N-pentanol sensor based on ZnO nanorods functionalized with Au catalysts. *Sens. Actuators B Chem.* **339**, 129888 (2021)
129. Rahimi, K., Yazdani, A.: Incremental photocatalytic reduction of graphene oxide on vertical ZnO nanorods for ultraviolet sensing. *Mater. Lett.* **262**, 127078 (2020)
130. Moon, S.H., et al.: van der Waals gap-inserted light-emitting p-n heterojunction of ZnO nanorods/graphene/p-GaN film. *Curr. Appl. Phys.* **20**(2), 352–357 (2020)
131. Mohammad, S.M., et al.: Ultraviolet electroluminescence from flowers-like n-ZnO nanorods/p-GaN light-emitting diode fabricated by modified chemical bath deposition. *J. Lumin.* **226**, 117510 (2020)
132. Abdelfatah, M., Ismail, W., El-Shaer, A.: Low cost inorganic white light emitting diode based on submicron ZnO rod arrays and electrodeposited Cu<sub>2</sub>O thin film. *Mater. Sci. Semicond. Process.* **81**, 44–47 (2018)
133. Ahmad, R., et al.: Recent progress and perspectives of gas sensors based on vertically oriented ZnO nanomaterials. *Adv. Coll. Interface. Sci.* **270**, 1–27 (2019)
134. Sadighbayan, D., Hasanzadeh, M., Ghafar-Zadeh, E.: Biosensing based on field-effect transistors (FET): recent progress and challenges. *TrAC Trends Anal. Chem.* **133**, 116067 (2020)
135. Tang, C., et al.: Facile synthesis and nanoscale related physical properties of core-shell structured CuO/ZnO nanorods on Si substrate. *Appl. Surf. Sci.* **509**, 144903 (2020)
136. Göktaş, S., Göktaş, A.: A comparative study on recent progress in efficient ZnO based nanocomposite and heterojunction photocatalysts: a review. *J. Alloys Compd.* **863**, 158734 (2021)
137. Sambath, K., et al.: Morphology controlled synthesis of ZnO nanostructures by varying pH. *J. Mater. Sci.: Mater. Electron.* **23**(2), 431–436 (2012)
138. Sinha, R., Roy, N., Mandal, T.K.: Growth of carbon dot-decorated ZnO nanorods on a graphite-coated paper substrate to fabricate a flexible and self-powered schottky diode for UV detection. *ACS Appl. Mater. Interfaces.* **12**(29), 33428–33438 (2020)
139. Lord, A.M., et al.: Schottky contacts on polarity-controlled vertical ZnO nanorods. *ACS Appl. Mater. Interfaces.* **12**(11), 13217–13228 (2020)
140. Nam, G.-H., Baek, S.-H., Park, I.-K.: Growth of ZnO nanorods on graphite substrate and its application for Schottky diode. *J. Alloy. Compd.* **613**, 37–41 (2014)
141. Pramanik, S., et al.: Role of oxygen vacancies on the green photoluminescence of microwave-assisted grown ZnO nanorods. *J. Alloys Compd.* **849**, 156684 (2020)
142. Efafi, B., et al.: Improvement in photoluminescence behavior of well-aligned ZnO nanorods by optimization of thermodynamic parameters. *Phys. B Condens. Matter* **579**, 411915 (2020)
143. Maldonado-Arriola, J., Sánchez-Zeferino, R., Álvarez-Ramos, M.: Photoluminescent properties of ZnO nanorods films used to detect methanol contamination in tequila. *Sensors. Actuators A Phys.* **312**, 112142 (2020)
144. Tamashevski, A., et al.: Photoluminescent detection of human T-lymphoblastic cells by ZnO nanorods. *Molecules* **25**(14), 3168 (2020)
145. Galdámez-Martínez, A., et al.: Photoluminescence of ZnO nanowires: a review. *Nanomaterials* **10**(5), 857 (2020)
146. Park, W.I., et al.: Excitonic emissions observed in ZnO single crystal nanorods. *Appl. Phys. Lett.* **82**(6), 964–966 (2003)
147. Shohany, B.G., Zak, A.K.: Doped ZnO nanostructures with selected elements-Structural, morphology and optical properties: a review. *Ceram. Int.* **46**(5), 5507–5520 (2020)
148. Gherab, K., et al.: Fabrication and characterizations of Al nanoparticles doped ZnO nanostructures-based integrated electrochemical biosensor. *J. Mark. Res.* **9**(1), 857–867 (2020)
149. Bhati, V.S., Hojamberdiev, M., Kumar, M.: Enhanced sensing performance of ZnO nanostructures-based gas sensors: A review. *Energy Rep.* **6**, 46–62 (2020)
150. Rehman, U., et al.: Modulation of secondary phases in hydrothermally grown zinc oxide nanostructures by varying the Cu dopant concentration for enhanced thermo power. *J. Alloys Compd.* **843**, 156081 (2020)
151. Tu, N., et al.: Effect of substrate temperature on structural and optical properties of ZnO nanostructures grown by thermal evaporation method. *Phys. E* **85**, 174–179 (2017)
152. Čížek, J., et al.: Origin of green luminescence in hydrothermally grown ZnO single crystals. *Appl. Phys. Lett.* **106**(25), 251902 (2015)
153. Huang, Z., et al.: Conversion mechanism of conductivity and properties of nitrogen implanted ZnO single crystals induced by post-annealing. *J. Mater. Sci. Mater. Electron.* **30**(5), 4555–4561 (2019)
154. Matsumoto, K., Kuriyama, K., Kushida, K.: Electrical and photoluminescence properties of carbon implanted ZnO bulk single crystals. *Nucl. Instrum. Methods Phys. Res. Sect. B* **267**(8–9), 1568–1570 (2009)
155. Richters, J.-P., et al.: Influence of polymer coating on the low-temperature photoluminescence properties of ZnO nanowires. *Appl. Phys. Lett.* **92**(1), 011103 (2008)
156. Liu, K., et al.: Photoluminescence characteristics of high quality ZnO nanowires and its enhancement by polymer covering. *Appl. Phys. Lett.* **96**(2), 023111 (2010)
157. Huang, M.H., et al.: Room-temperature ultraviolet nanowire nanolasers. *Science* **292**(5523), 2001 (1897)
158. Zhang, X., et al.: Structure and optically pumped lasing from nanocrystalline ZnO thin films prepared by thermal oxidation of ZnS thin films. *J. Appl. Phys.* **92**(6), 3293–3298 (2002)
159. Choy, J.H., et al.: Soft solution route to directionally grown ZnO nanorod arrays on Si wafer; room-temperature ultraviolet laser. *Adv. Mater.* **15**(22), 1911–1914 (2003)
160. Yu, S., et al.: Random laser action in ZnO nanorod arrays embedded in ZnO epilayers. *Appl. Phys. Lett.* **84**(17), 3241–3243 (2004)
161. Lorenz, M., et al.: Cathodoluminescence of selected single ZnO nanowires on sapphire. *Ann. Phys.* **13**(1–2), 39–42 (2004)
162. Teng, F., et al.: Photoelectric detectors based on inorganic p-type semiconductor materials. *Adv. Mater.* **30**(35), 1706262 (2018)
163. Yu, J., et al.: Metal-free carbon materials for persulfate-based advanced oxidation process: Microstructure, property and tailoring. *Progress Mater. Sci.* **111**, 100654 (2020)
164. Kurilich, M.R., et al.: Comparative study of electron field emission from randomly-oriented and vertically-aligned carbon nanotubes synthesized on stainless steel substrates. *J. Vac. Sci. Technol. B Nanotechnol. Microelectron. Mater. Process. Meas. Phenom* **37**(4), 041202 (2019)
165. Chen, B., et al.: Length effect of carbon nanotubes on the strengthening mechanisms in metal matrix composites. *Acta Mater.* **140**, 317–325 (2017)
166. Lee, C.J., et al.: Field emission from well-aligned zinc oxide nanowires grown at low temperature. *Appl. Phys. Lett.* **81**(19), 3648–3650 (2002)
167. Park, W.I., Yi, G.C.: Electroluminescence in n-ZnO nanorod arrays vertically grown on p-GaN. *Adv. Mater.* **16**(1), 87–90 (2004)



168. Kennedy, J., et al.: Synthesis and enhanced field emission of zinc oxide incorporated carbon nanotubes. *Diam. Relat. Mater.* **71**, 79–84 (2017)
169. Chikate, P.R., et al.: Spitzer shaped ZnO nanostructures for enhancement of field electron emission behaviors. *RSC Adv.* **8**(38), 21664–21670 (2018)
170. Young, S.-J., Liu, Y.-H., Chien, J.-T.: Improving field electron emission properties of ZnO nanosheets with Ag nanoparticles adsorbed by photochemical method. *ACS Omega* **3**(7), 8135–8140 (2018)
171. Dalvand, R., et al.: Well-aligned ZnO nanoneedle arrays grown on polycarbonate substrates via electric field-assisted chemical method. *Mater. Lett.* **146**, 65–68 (2015)
172. Li, S.Y., et al.: Field emission and photofluorescent characteristics of zinc oxide nanowires synthesized by a metal catalyzed vapor-liquid-solid process. *J. Appl. Phys.* **95**(7), 3711–3716 (2004)
173. Pan, N., et al.: Tip-morphology-dependent field emission from ZnO nanorod arrays. *Nanotechnology* **21**(22), 225707 (2010)
174. Li, Y., Bando, Y., Golberg, D.: ZnO nanoneedles with tip surface perturbations: excellent field emitters. *Appl. Phys. Lett.* **84**(18), 3603–3605 (2004)
175. Xu, C., Sun, X.: Field emission from zinc oxide nanopins. *Appl. Phys. Lett.* **83**(18), 3806–3808 (2003)
176. Maiti, S., Pal, S., Chattopadhyay, K.K.: Recent advances in low temperature, solution processed morphology tailored ZnO nanoarchitectures for electron emission and photocatalysis applications. *CrystEngComm* **17**(48), 9264–9295 (2015)
177. Maiti, S., et al.: Ambient condition oxidation of zinc foil in supersaturated solution for shape tailored ZnO nanostructures: low cost candidates for efficient electron emitter and UV-detector. *CrystEngComm* **16**(9), 1659–1668 (2014)
178. Jaramillo-Cabanzo, D., et al.: One-dimensional nanomaterials in lithium-ion batteries. *J. Phys. D Appl. Phys.* **54**(8), 083001 (2020)
179. Jo, S., et al.: Field-emission studies on thin films of zinc oxide nanowires. *Appl. Phys. Lett.* **83**(23), 4821–4823 (2003)
180. Xu, C., Sun, X., Chen, B.: Field emission from gallium-doped zinc oxide nanofiber array. *Appl. Phys. Lett.* **84**(9), 1540–1542 (2004)
181. Yoo, J., Park, W.I., Yi, G.-C.: Electrical and optical characteristics of hydrogen-plasma treated ZnO nanoneedles. *J. Vac. Sci. Technol. B Microelectron. Nanometer Struct. Process. Meas. Phenom.* **23**(5), 1970–1974 (2005)
182. Liu, Y., et al.: Nature-inspired structural materials for flexible electronic devices. *Chem. Rev.* **117**(20), 12893–12941 (2017)
183. Wang, Z., et al.: Nanoionics-enabled memristive devices: strategies and materials for neuromorphic applications. *Adv. Electron. Mater.* **3**(7), 1600510 (2017)
184. Singh, P., et al.: Sensing performance of gas sensors fabricated from controllably grown ZnO-based nanorods on seed layers. *J. Mater. Sci.* **55**(21), 8850–8860 (2020)
185. Wang, J., et al.: Room-temperature gas sensors based on ZnO nanorod/Au hybrids: visible-light-modulated dual selectivity to NO<sub>2</sub> and NH<sub>3</sub>. *J. Hazard. Mater.* **381**, 120919 (2020)
186. Kasapoğlu, A.E., et al.: The effect of the change in the amount of Sb doping in ZnO nanorods for hydrogen gas sensors. *Int. J. Hydrogen Energy* **46**(41), 21715–21725 (2021)
187. Zhao, S., et al.: Enhanced NO<sub>2</sub> sensing performance of ZnO nanowires functionalized with ultra-fine In<sub>2</sub>O<sub>3</sub> nanoparticles. *Sens. Actuators B Chem.* **308**, 127729 (2020)
188. Miao, J., Lin, J.Y.: Nanometer-thick films of aligned ZnO nanowires sensitized with Au nanoparticles for few-ppb-level acetylene detection. *ACS Appl. Nano Mater.* **3**(9), 9174–9184 (2020)
189. Gole, A., Murphy, C.J.: Biotin–streptavidin-induced aggregation of gold nanorods: tuning rod–rod orientation. *Langmuir* **21**(23), 10756–10762 (2005)
190. Husham, M., et al.: Synthesis of ZnO nanorods by microwave-assisted chemical-bath deposition for highly sensitive self-powered UV detection application. *Sens. Actuators, A* **263**, 166–173 (2017)
191. Hahm, J.-I.: Zinc oxide nanomaterials for biomedical fluorescence detection. *J. Nanosci. Nanotechnol.* **14**(1), 475–486 (2014)
192. Willander, M., Khun, K., Ibutopo, Z.H.: ZnO based potentiometric and amperometric nanosensors. *J. Nanosci. Nanotechnol.* **14**(9), 6497–6508 (2014)
193. Sun, X., et al.: Shape controllable synthesis of ZnO nanorod arrays via vapor phase growth. *Solid State Commun.* **129**(12), 803–807 (2004)
194. Ahn, S.E., et al.: Photoresponse of sol-gel-synthesized ZnO nanorods. *Appl. Phys. Lett.* **84**(24), 5022–5024 (2004)
195. Park, W.I., et al.: Schottky nanocontacts on ZnO nanorod arrays. *Appl. Phys. Lett.* **82**(24), 4358–4360 (2003)
196. Chang, H., et al.: Facile fabrication of self-assembled ZnO nanowire network channels and its gate-controlled UV detection. *Nanoscale Res. Lett.* **13**(1), 1–9 (2018)
197. Yang, Y., et al.: Transverse piezoelectric field-effect transistor based on single ZnO nanobelts. *Phys. Chem. Chem. Phys.* **12**(39), 12415–12419 (2010)
198. Park, W.I., et al.: Fabrication and electrical characteristics of high-performance ZnO nanorod field-effect transistors. *Appl. Phys. Lett.* **85**(21), 5052–5054 (2004)
199. Wang, H.-T.: Fabrication and Characterization of Zinc Oxide and Gallium Nitride Based Sensors. University of Florida (2008)
200. Abdulrahman, A.F., et al.: Effect of growth temperature on morphological, structural, and optical properties of ZnO nanorods using modified chemical bath deposition method. *J. Electron. Mater.* **50**(3), 1482–1495 (2021)
201. Costas, A., et al.: Photodetecting properties of single CuO–ZnO core–shell nanowires with p–n radial heterojunction. *Sci. Rep.* **10**(1), 1–12 (2020)
202. Wan, Q., et al.: Fabrication and ethanol sensing characteristics of ZnO nanowire gas sensors. *Appl. Phys. Lett.* **84**(18), 3654–3656 (2004)

**Publisher's Note** Springer Nature remains neutral with regard to jurisdictional claims in published maps and institutional affiliations.